Simultaneous K-Plus-L-Shell Ionization in Light-Ion-Atom Collisions*

T. K. Li, R. L. Watson, and J. S. Hansen
Department of Chemistry and Cyclotron Institute, Texas A&M University, College Station, Texas 77843
(Received 11 December 1972)

The probability of simultaneous K-plus-L-shell ionization in collisions between Ca, Ti, and Fe target atoms and projectiles of 1.5 – 12.5-MeV/amu deuterons and α particles has been investigated. The results show that the fraction of $K\beta$ x rays emitted in the presence of an L-shell vacancy (a) decreases with increasing projectile velocity above a projectile-to-L-shell-electron velocity ratio of 1; (b) decreases with increasing target atomic number; and (c) increases with projectile charge (approximately as z_1^2). The projectile velocity dependence is in fairly good agreement with a simple classical model based upon the assumption that multiple-vacancy production results from simultaneous Coulomb collisions with K- and L-shell electrons during the ion's passage through the atom.

I. INTRODUCTION

Numerous studies of ion-atom collisions have been reported in which it has been shown that K-shell ionization is usually accompanied by multiple L-shell ionization when fast heavy ions ($Z > 2$) are used as projectiles.[1] Recently, simultaneous K-plus-L-shell ionization has also been observed in fast-proton and α-particle collisions.[2-4] An examination of the intensities of multiple ionization satellites appearing in high-resolution crystal spectrometer spectra of Al K x rays following He-ion excitation, by Knudson, Burkhalter, and Nagel,[2] has indicated that the mechanism involved is that of direct multiple Coulomb excitation.

We report here the results of an extensive study of the velocity dependence of the simultaneous K-plus-L-shell ionization process using 1.5–12.5-MeV/amu deuterons and α-particles incident on targets of Ca, Ti, and Fe. In this work, simultaneous K-plus-L-shell ionization probabilities were deduced from measurements of $K\beta$-to-$K\alpha$ x-ray intensity ratios by taking advantage of a critical absorption effect.

Our interest in studying the multiple ionization process with light, fully stripped ions is associated with the expectation that a rigorous theoretical treatment of this problem should be much simpler than for multiple ionization resulting from heavy-ion–atom collisions where quasimolecular structure effects may play an important role. A classical description of multiple ionization in light-ion collisions was given some time ago by Gryzinski.[5] Recently, other more detailed semiclassical approaches have been applied to the problem.[6,7] In the present analysis we have investigated the extent to which a simplified treatment of the problem, in terms of easily calculable analytical expressions, is capable of reproducing the projectile energy dependence of the simultaneous K-plus-L-shell ionization probability.

II. EXPERIMENTAL DESCRIPTION

A. Method

The experimental technique used in the present work is based upon the fact that a $K\beta$ x ray emitted in the presence of an L-shell vacancy has a higher energy than a "normal" $K\beta$ x ray (i.e., one emitted from an atom containing only a K-shell vacancy). If the shifted $K\beta$ x-ray energy is greated than the K binding energy of the ground-state atom, those $K\beta$ x rays emitted from atoms which have an L-shell vacancy remaining as a result of simultaneous K-plus-L-shell ionization during the collision process will suffer critical absorption in passing through a substance containing atoms of the same element as the target. Such a situation is illustrated in Fig. 1, where the mass absorption coefficient for Ti[8] as a function of photon energy is shown. The transmission of a shifted Ti $K\beta$ x ray of energy $E'_{K\beta}$ through a 4-mg/cm^2 Ti absorber, for example, is only 6% as compared to 71% for a normal Ti $K\beta$ x ray of energy $E_{K\beta}$. The small energy shift experienced by a Ti $K\alpha$ x ray emitted in the presence of an L-shell vacancy, on the other hand, does not significantly alter its transmission relative to a normal $K\alpha$ x ray. Thus, by measuring the intensity of $K\beta$ x rays relative to the intensity of $K\alpha$ x rays with and without an absorber, it is possible to determine the fraction of $K\beta$ x rays emitted in the presence of an L-shell vacancy for elements in which the $K\beta$ x-ray energy shift is sufficient to cause critical absorption.

A formulation of this method is as follows: Let g_{KL} equal the fraction of $K\beta$ x rays emitted in the presence of one or more L-shell vacancies, f_n^B (or

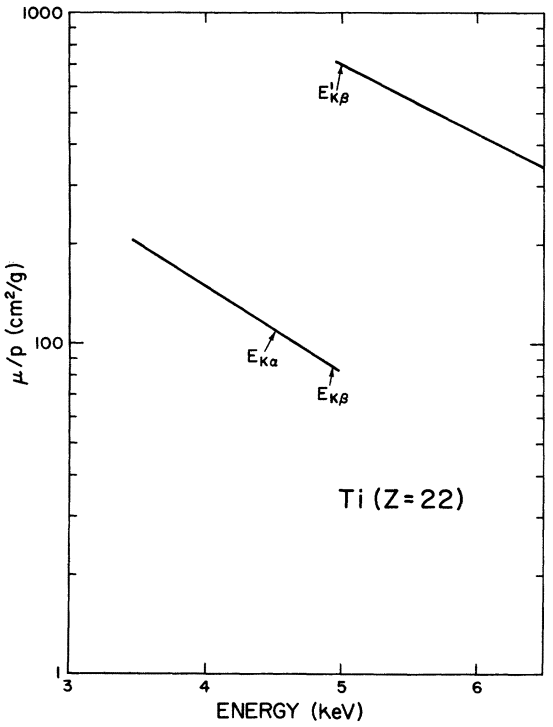

FIG. 1. Total mass absorption coefficient for Ti as a function of photon energy. The arrows indicate the positions of the normal Ti $K\alpha$ and $K\beta$ x rays ($E_{K\alpha}$ and $E_{K\beta}$) and of the shifted $K\beta$ x rays ($E'_{K\beta}$).

f_n^α) is the transmission probability of *normal* $K\beta$ (or $K\alpha$) x rays through an absorber; f_s^β is the transmission probability of *shifted* $K\beta$ x rays through an absorber; I_β^0 (or I_α^0) is the total emitted intensity of $K\beta$ (or $K\alpha$) x rays; I_β (or I_α) is the total transmitted intensity of $K\beta$ (or $K\alpha$) x rays. Then

$$(I_\beta/I_\alpha)\,\text{(with absorber)} = [I_\beta^0 g_{KL} f_s^\beta + I_\beta^0(1-g_{KL}) f_n^\beta]/I_\alpha^0 f_n^\alpha$$

and

$$(I_\beta/I_\alpha)\,\text{(without absorber)} = I_\beta^0/I_\alpha^0 .$$

Now

$$R \equiv \frac{(I_\beta/I_\alpha)\,\text{(with absorber)}}{(I_\beta/I_\alpha)\,\text{(without absorber)}} = \frac{g_{KL} f_s^\beta + (1-g_{KL}) f_n^\beta}{f_n^\alpha},$$

so

$$g_{KL} = \frac{f_n^\beta - R f_n^\alpha}{f_n^\beta - f_s^\beta} . \qquad (1)$$

If the $K\beta$ fluorescence yield does not change significantly as a result of the presence of an L-shell vacancy and if the lifetime of an L-shell vacancy is long compared to the lifetime of a K-shell vacancy, then

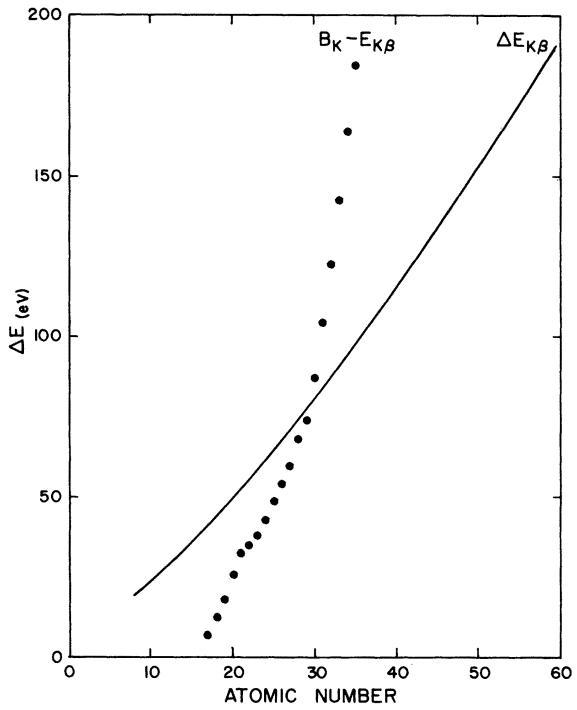

FIG. 2. Comparison of the calculated $K\beta$ x-ray energy shift for K x-ray emission in the presence of a single L-shell vacancy, $\Delta E_{K\beta}$, with the difference between the normal K-shell binding energy and the normal $K\beta$ x-ray energy, $B_K - E_{K\beta}$. Those elements for which $\Delta E_{K\beta} > B_K - E_{K\beta}$ should display the critical absorption effect.

$$g_{KL} \simeq P_{KL} \equiv \sigma_{KL}/\sigma_K , \qquad (2)$$

where P_{KL} is the probability of simultaneous K-plus-L-shell ionization, σ_K is the total K-shell ionization cross section, and σ_{KL} is the cross section for producing *at least* one L-shell vacancy simultaneously with a K-shell vacancy. The assumptions involved in equating g_{KL} to P_{KL} will be discussed in more detail in Sec. III.

We have carried out hfs calculations of $K\beta$ x-ray energy shifts for atoms having a single L-shell vacancy in addition to a K-shell vacancy using the program of Herman and Skillman.[9] The results of these calculations are shown in Fig. 2, where the calculated $K\beta$ x-ray energy shift $\Delta E_{K\beta}$ is compared to the energy difference between the K-shell binding energy and the normal $K\beta$ x-ray energy, $B_K - E_{K\beta}$. Those elements for which $\Delta E_{K\beta} > B_K - E_{K\beta}$ are expected to display the critical absorption effect. It is seen in Fig. 2 that the critical absorption technique should be applicable to elements having $Z \leq 29$.

The aforementioned conclusion was checked in a preliminary experiment[3] which compared the $K\beta$-to-$K\alpha$ intensity ratios measured with 2.88-MeV/amu α particles incident on relatively thick targets (~7 mg/cm^2) of elements from $Z = 22$ to

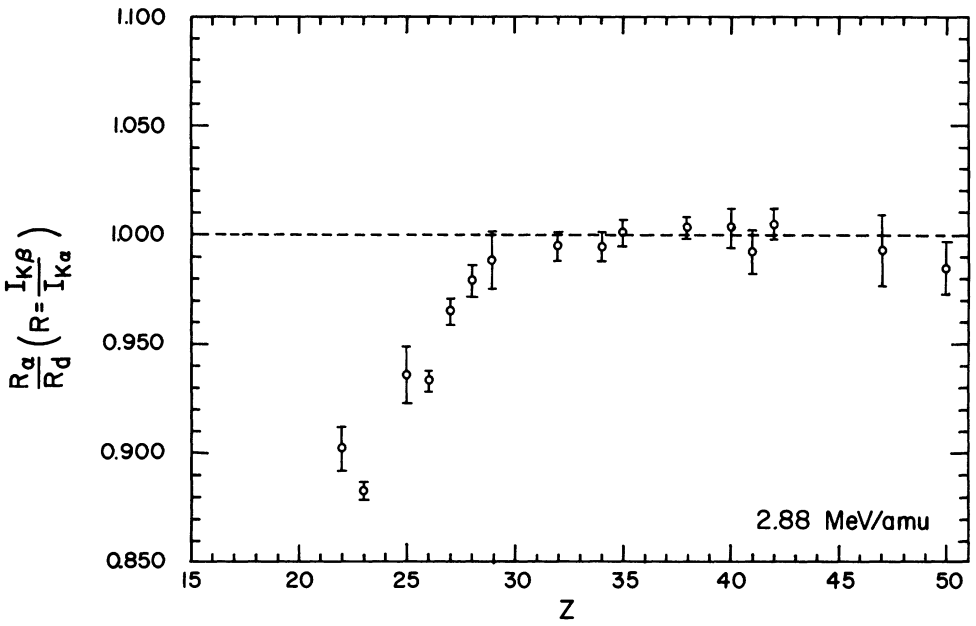

FIG. 3. Ratio R_α/R_d as a function of target atomic number, where R_α is the thick-target $K\beta$-to-$K\alpha$ x-ray intensity ratio measured with α particles as projectiles, and R_d is the same quantity measured with equal velocity deuterons as projectiles. The decrease in R_α/R_d beginning near $Z = 30$ is due to critical absorption of shifted $K\beta$ x rays in the target.

50 with the $K\beta$-to-$K\alpha$ intensity ratios obtained with equal-velocity deuterons. The results are shown in Fig. 3, where the $K\beta$-to-$K\alpha$ intensity ratio for α-particle excitation, R_α, divided by the $K\beta$-to-$K\alpha$ intensity ratio for deuteron excitation, R_d, is plotted versus target atomic number. The abrupt dip in the ratio below $Z \simeq 30$ is interpreted as resulting from the onset of the critical absorption effect just described. The probability of simultaneous K-plus-L-shell ionization is expected to be larger for α-particle collisions than for deuteron collisions because of the relative charges involved, and so the ratio R_α should be smaller than the ratio R_d when critical absorption of shifted $K\beta$ x rays occurs in the target. The data shown in Fig. 3 are consistent with this prediction and the onset of the decrease in R_α/R_d near $Z = 30$ is in good agreement with the calculated $K\beta$ x-ray energy shifts.

B. Procedure and Analysis

The experimental arrangement including the beam transport system, target chamber, and x-ray spectrometer was similar to that described previously.[10] Beams of deuterons and α-particles having energies of 1.50, 2.33, 2.88, 3.88, 4.25, 6.25, 7.50, 10.0, and 12.5 MeV/amu were extracted from the Texas A&M variable energy cyclotron and focused onto targets mounted at a 45° angle with respect to both the incident beam and the x-ray spectrometer. The x-ray spectrometer was a Si(Li) detector system positioned at 90° to the incident beam and separated from the target chamber by a 52-mg/cm^2 beryllium window. The resolution of the x-ray spectrometer was 250 eV full width at half-maximum at 6.4 keV.

Target elements of Ca ($Z = 20$), Ti ($Z = 22$), and Fe ($Z = 26$) were used. Thin targets were vacuum evaporated onto 520-μg/cm^2 Mylar backings. Taking into account the 45° inclination angle, the effective thicknesses of the targets were 35 μg/cm^2 for Ca (in the form of CaF_2), 35 μg/cm^2 for Ti (metal), and 41 μg/cm^2 for Fe (metal). The thicknesses of the absorbers used in these experiments were 0.86 mg/cm^2 for Ca (CaF_2 vacuum evaporated onto a 520 μg/cm^2 Mylar backing), 3.09 mg/cm^2 for Ti (self-supported foil), and 2.18 mg/cm^2 for Fe (self-supported foil). These thicknesses were sufficient to cause absorption of 59, 89, and 59% of the Ca-, Ti-, and Fe-shifted $K\beta$ x rays, respectively.

X-ray spectra were recorded sequentially with and without an absorber positioned in front of the x-ray-spectrometer entrance window using first one beam and then the other at each energy. Usually, three sets of spectra were measured for each target in a run with a given projectile. During the course of this work, an average of two runs per projectile were made at each energy.

All of the x-ray spectra were carefully analyzed with a least-squares peak fitting computer program[11] from which the $K\alpha$ and $K\beta$ x-ray group intensities were determined. The reliability of this peak fitting procedure for the accurate determination of peak intensities has been discussed

TABLE I. Experimental values of g_{KL}, the fraction of K x rays emitted in the presence of an L-shell vacancy.

Projectile	Energy (MeV/amu)	$100\times g_{KL}$ Ca	Ti	Fe
deuterons	1.50	8.0±1.3	7.0±0.8	5.4±0.9
	2.33	6.7±1.3	6.8±1.0	5.0±0.6
	2.88	5.4±1.1	6.1±0.7	4.1±0.6
	3.88		5.0±0.7	3.6±0.9
	4.25		4.1±0.7	3.5±0.7
	6.25	3.6±1.1	2.9±0.4	2.8±0.8
	7.50	2.6±0.7	2.8±0.6	2.6±0.7
	10.00	2.4±1.0	2.4±0.9	1.9±0.7
	12.50	1.7±0.7	1.8±0.5	1.5±0.6
α particles	1.50	29.2±1.4	26.3±0.5	19.6±0.7
	2.33	24.4±2.0	22.1±0.8	17.6±0.6
	2.88	18.5±1.4	21.7±0.9	16.7±0.7
	3.88		18.9±0.8	13.9±0.8
	4.25		13.2±0.7	12.0±0.6
	6.25	10.2±0.8	11.0±0.4	10.0±0.7
	7.50	9.1±1.0	10.5±0.8	9.4±0.7
	10.00	7.1±0.6	9.2±0.7	6.6±0.7
	12.50	6.0±0.7	7.9±0.6	5.3±0.7

elsewhere.[12,13] In the calculation of g_{KL} values with Eq. (1), absorption coefficients from the tabulation by Storm and Israel[8] were used.

III. RESULTS AND DISCUSSION

The experimental g_{KL} values for simultaneous K-plus-L-shell ionization of Ca, Ti, and Fe with 1.5–12.5-MeV/amu deuterons and α-particles are presented in Table I. The errors listed for these g_{KL} values were obtained from the root-mean-square deviations of three or more independent determinations of the $K\beta$-to-$K\alpha$ x-ray intensity ratios involved. They do not take into account error due to absorber nonuniformity or uncertainty in the absorption coefficients. Inaccuracies of 10% in both of these quantities will alter the values of g_{KL} for Ca by 6%, for Ti by 4%, and for Fe by 7%, on the average. The data are shown in Fig. 4 plotted as a function of projectile energy per amu. In this figure it is observed that the g_{KL} values (a) decrease as the projectile energy increases, (b) decrease as the target atomic number increases, and (c) increase as the projectile charge increases (approximately as z_1^2).

In an attempt to characterize the velocity dependence of the simultaneous K-plus-L-shell ionization probability, in terms of easily calculable analytical expressions, we have employed a simple model based upon the assumption that multiple vacancy production in light-ion collisions is the result of simultaneous Coulomb collisions with K- and L-shell electrons during the ion's passage through the atom. Consider only those collisions for which K-shell ionization has a maximum probability (i.e., impact parameters of the order of magnitude of the K-shell radius). For charged particles passing near the K-shell radius of the target, we take the quantity

$$p_L = k(Z)\hat{\sigma}_L \tag{3}$$

as the probability per electron, p_L, of ionizing an L-shell electron, where $\hat{\sigma}_L$ is the L-shell ionization cross section per electron. We shall (somewhat arbitrarily) set the proportionality constant $k(Z)$ equal to $1/\pi\langle r_L^2\rangle$, where $\langle r_L^2\rangle$ is the mean-square radius of the L-shell of the target atom. This choice for $k(Z)$ is equivalent to assuming (a) that all K-shell ionizing collisions occur at impact parameters smaller than the mean L-shell radius, and (b) that the L-shell ionization cross section remains constant over this region. The total probability of ionizing, *at least*, one L-shell electron, P_L, in such a collision may be written as

$$P_L = 1-(1-p_L)^{n_L}, \tag{4}$$

where n_L is the total number of L-shell electrons. Now, the total cross section for K-shell ionization accompanied by one or more L-shell ionizations is given by

$$\sigma_{KL} = \sigma_K P_L, \tag{5}$$

where σ_K is the total cross section for K-shell ionization. Hence,

$$P_{KL} = \sigma_{KL}/\sigma_K = P_L . \tag{6}$$

We have used the results of the classical description of ionization by Gryzinski[5] to calculate the L-shell ionization cross section needed in Eq. (3). Accordingly, the ionization cross section is given by

$$\hat{\sigma}_n = (\pi z_1^2 e^4/\langle U_n^2\rangle) G_n(v_1/\bar{v}_n), \tag{7}$$

where $\langle U_n^2\rangle$ and $\bar{v}_n$ are the average squared binding energy and average velocity of an orbital electron in the n shell, z_1 and v_1 are the charge and velocity of the projectile, and $G_n(v_1/\bar{v}_n)$ is given by

$$G_n(v_1/\bar{v}_n) = G_n(y) = f(y)\left[\frac{y^2}{1+y^2} + \tfrac{2}{3}\left(1+\frac{1}{\alpha}\right)\ln(2.7+y)\right] \times\left[1-\frac{1}{\alpha}\right]\left[1-\left(\frac{1}{\alpha}\right)^{1+y^2}\right] \tag{8}$$

in which

$$\alpha = 4y^2(1+1/y)$$

and

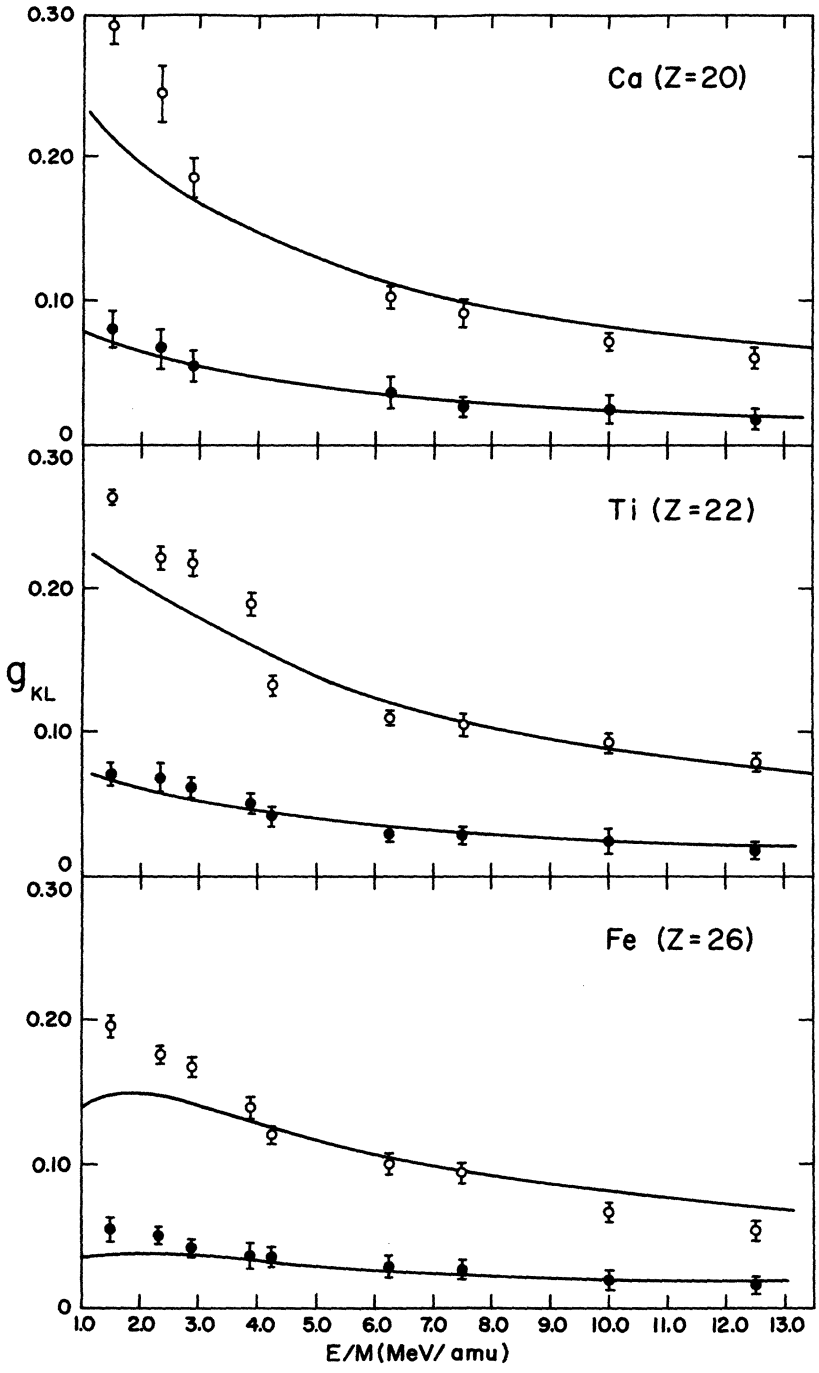

FIG. 4. Experimental g_{KL} values for Ca, Ti, and Fe plotted vs projectile energy per amu. The open circles are for α particles and the closed circles are for deuterons. The normalized results of the simplified model analysis employing the Gryzinski formula for ionization by Coulomb excitation are shown by the solid curves.

$$f(y) = \frac{1}{y^2}\left(\frac{y^2}{1+y^2}\right)^{3/2}.$$

Therefore

$$p_L \simeq \frac{\hat{\sigma}_L}{\langle r_L^2\rangle} = \frac{z_1^2 e^4}{\langle U_L^2\rangle \langle r_L^2\rangle} G_L(v_1/\bar{v}_L). \tag{9}$$

The predictions of this simple analysis are shown by the solid curves in Fig. 4. The values of $\langle U_L\rangle$, $\langle U_L^2\rangle$, and $\langle r_L^2\rangle$ used in computing p_L are listed in Table II. In each case, the averages were obtained by weighting the $2s$ and $2p$ subshells by factors of 2 and 6, respectively. Values of $\langle r^2\rangle$ were calculated for the $2s$ and $2p$ subshells using the hfs program of Herman and Skillman,[9] and average L-electron velocities were computed from the virial theorem ($\bar{v}_L = (2\langle U_L\rangle m)^{1/2}$, where m is the electron mass). The solid curves in Fig. 4

TABLE II. Average L-shell binding energies and radii used in calculating P_{KL}.

Element	$\langle U_L \rangle$ [a] (keV)	$\langle U_L^2 \rangle$ (keV^2)	$\langle r_L^2 \rangle$ [b] (10^{-18} cm^2)
$_{20}$Ca	0.362	0.139	3.79
$_{22}$Ti	0.475	0.236	2.99
$_{26}$Fe	0.749	0.563	2.00

[a] Taken from a compilation by Bearden and Burr (Ref. 21).

[b] Calculated using the hfs program of Herman and Skillman (Ref. 9).

have been normalized to the data points by multiplying the theoretical values by 0.55 in the case of Ca, by 0.64 in the case of Ti, and by 0.62 in the case of Fe.

It is seen that the energy dependence of the experimental g_{KL} values is fairly well represented by the simple analysis just described, except at low energies where the theoretical curves tend to fall somewhat below the experimental data. In the case of Fe, the Gryzinski formula predicts a maximum at about 2 MeV/amu, but the experimental data do not extend to low enough energies to check this feature.

Quite recently, Hansen[7] has carried out a formulation of the binary-encounter approximation in an impact-parameter representation and has applied it to the calculation of simultaneous K-plus-L-shell ionization probabilities. The calculation determines P_{KL} from an explicit average of the L-shell ionization probability over impact parameters which lead to K-shell ionization. In Fig. 5, the results of these calculations for Ti are compared with the experimental data and with the analysis just described. None of the curves shown in Fig. 5 have been normalized. The results of Hansen's BEA treatment are quite similar to those of the present simplified treatment except in the low-energy region, where it is seen that the Hansen curve begins turning over sooner than does the curve calculated from the Gryzinski formula. The apparent over-all agreement between the magnitudes of the P_{KL} values predicted by the two methods is merely a result of our fortuitous choice of $1/\pi \langle r_L^2 \rangle$ for the proportionality constant in Eq. (3).

In Fig. 6, the Hansen calculations for Fe are compared to the experimental data and to the results of a recent semiclassical calculation by Hansteen and Mosebekk[6] for protons on Cu. It appears that the SCA calculations predict an energy dependence which is very different from that displayed by the experimental measurements and from the results of the BEA calculations.

It is important to recognize the fact that x-ray measurements, in general, do not provide direct information relating to the state of excitation which is produced at the time of collision. In the case of the present experiments, for example, one must keep in mind that g_{KL} is the fraction of $K\beta$ x rays emitted in the presence of one or more L-shell vacancies, whereas P_{KL} is the fraction of K-shell ionizations accompanied by one or more L-shell ionizations. Hence, if atomic rearrangement occurs to any significant extent prior to deexcitation via $K\beta$ x-ray emission, the relationship between g_{KL} and P_{KL} will be considerably altered from

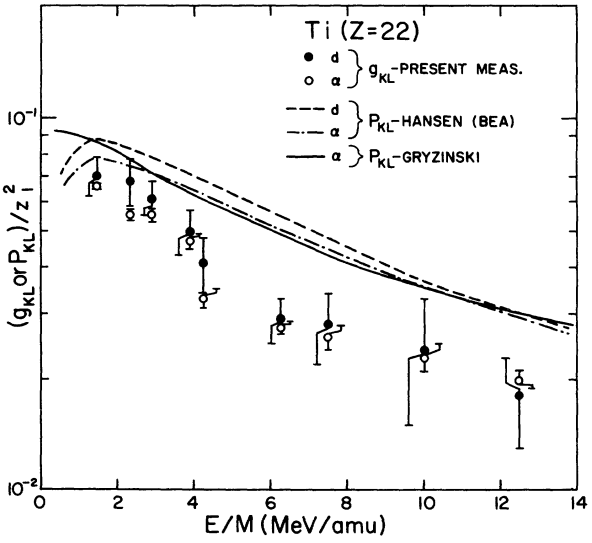

FIG. 5. Comparison of the experimental g_{KL} values for Ti with the theoretical P_{KL} values calculated by Hansen (Ref. 7) and by the present method (Gryzinski).

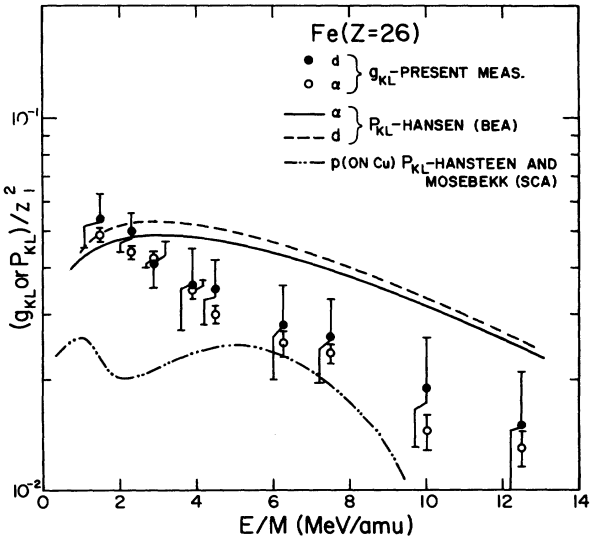

FIG. 6. A comparison of the experimental g_{KL} values for Fe with the theoretical P_{KL} values calculated by Hansen (Ref. 7) and with the P_{KL} values calculated for protons on Cu by Hansteen and Mosebekk (Ref. 6).

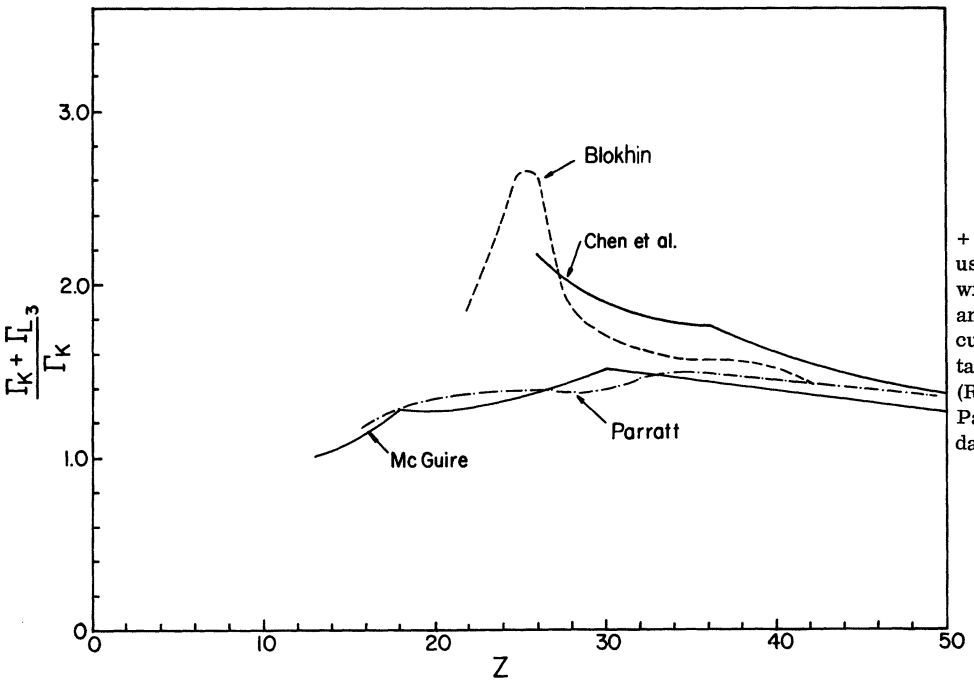

FIG. 7. The factor $(\Gamma_K + \Gamma_{L_3})/\Gamma_K$ as determined using the theoretical level widths of McGuire (Ref. 14) and Chen (Ref. 15) (solid curves) and the experimental level widths of Blokhin (Ref. 19) (dashed curve) and Parratt (Ref. 20) (dot-dashed curve).

that given in Eq. (2). A detailed analysis of this problem is given in the Appendix for the special case in which simultaneous multiple L-shell ionization is sufficiently improbable that it may be neglected. It is found that, to a good approximation, g_{KL} and P_{KL} are related by the equation

$$P_{KL} \simeq [(\Gamma_K + \Gamma_{L_3})/\Gamma_K]\, g_{KL}, \tag{10}$$

where Γ_K is the total K-shell level width and Γ_{L_3} is the level width of the L_3 subshell. This equation will overestimate P_{KL} when multiple L-shell ionization occurs to a significant extent since, in this case, one of the L-shell vacancies can decay away and a shifted $K\beta$ x ray could still be emitted. With regard to the present data, we believe that the neglect of multiple L-shell ionization is justified on the basis of a high-resolution x-ray spectral measurement carried out by Moore *et al.*[4] using 3.2-MeV α particles incident on Ti. In the spectrum presented by these investigators, we note that the ratio of the K-plus-double-L-shell ionization $K\alpha$-satellite-peak intensity to the total $K\alpha$ intensity is only about 0.02, while the ratio of the K-plus-single-L-shell ionization $K\alpha$-satellite-peak intensity to the total $K\alpha$ intensity is about 0.2.

The factor $(\Gamma_K + \Gamma_{L_3})/\Gamma_K$, as determined from various theoretical and experimental values of Γ_{L_3}, is shown plotted as a function of atomic number in Fig. 7. The solid curves appearing in this figure were computed using the adjusted theoretical L_2 (for $Z \leq 12$) and L_3 (for $Z \geq 20$) level widths of McGuire,[14] and the theoretical L_3 level widths of Chen *et al.*[15] The K-shell level widths used in constructing both of these curves were computed from the theoretical K-shell radiative widths of Scofield[16] and the semiempirical K-shell fluorescence yield values obtained from Bambynek *et al.*[17] Level widths for the L-shell have also been calculated by Walters and Bhalla,[18] and their values are very nearly the same as McGuire's. The dashed curve in Fig. 7 was computed from the experimental L_3 level widths of Blokhin[19] and the dot-dashed curve was computed from the experimental L_3 level widths of Parratt.[20] The K-shell level widths used in constructing these two curves were taken from the experimental measurements of Blokhin.[19] It is seen that considerable disagreement exists among both the theoretical and experimental determinations of $(\Gamma_K + \Gamma_{L_3})/\Gamma_K$. The values of $(\Gamma_K + \Gamma_{L_3})/\Gamma_K$ which are required to normalize the present experimental data to the curves calculated by Hansen[7] are 1.60, 1.56, and 1.52, respectively, for Ca, Ti, and Fe.

One final comment relates to the effect of simultaneous M-shell ionization on the relationship between g_{KL} and P_{KL}. Undoubtedly, simultaneous M-shell ionization is considerably more probable than simultaneous L-shell ionization; however, the degree of M-shell ionization in atoms which have undergone simultaneous K-plus-L-shell ionization should be just about the same as the degree of M-shell ionization in atoms which have undergone K-shell ionization without simultaneous L-shell ionization. Therefore, the net effect of M-shell ionization, insofar as the relationship between g_{KL} and P_{KL} is concerned, will be to decrease

Γ_{L_3} with respect to Γ_K. In this event, Eq. (10) will again tend to overestimate P_{KL}.

In conclusion, then, we have shown that the projectile energy dependence of simultaneous K-plus-L-shell ionization in fast light-ion–atom collisions can be fairly well characterized in terms of a simplified classical model which employs an easily calculable analytical expression given by Gryzinski for ionization by Coulomb excitation. In addition, the effects of atomic rearrangement following the collision process have been examined. It is apparent that the deduction of accurate multiple L-shell ionization probabilities from x-ray or Auger-electron measurements will be a difficult task owing to the lack of information on atomic rearrangement rates.

ACKNOWLEDGMENTS

We acknowledge helpful discussions with Dr. J. H. McGuire regarding the application of the Gryzinski model to this work. The assistance of the Texas A & M cyclotron operations personnel was greatly appreciated.

APPENDIX: DERIVATION OF RELATIONSHIP BETWEEN P_{KL} AND g_{KL} FOR THE CASE OF SINGLE-K-PLUS-SINGLE-L-SHELL IONIZATION

Suppose there are N_K^0 target atoms having a single K-shell vacancy and N_{KL}^0 target atoms having a single-K-plus-single-L-shell vacancy at time $t=0$. At any subsequent time t, some of these initial states will have decayed to new states via x-ray and Auger transitions. The various states which would be formed in appreciable amounts as a result of these decay processes are summarized for elements in the region of Ca to Fe[17,18]:

Initial state — Final states

$K \xrightarrow{\lambda_K} L, M, LL, LM, MM$

$KL \xrightarrow{\lambda'_K} LL, LM, LLL, LLM, LMM$

$KL \xrightarrow{\lambda'_L} KMM \xrightarrow{\lambda''_K} LMM, MMM, LLMM, LMMM, MMMM.$

The various sources of $K\beta$ x rays are summarized as follows:

Initial state		Final state
K	$\xrightarrow{\lambda_{K\beta}}$	M
KL	$\xrightarrow{\lambda'_{K\beta}}$	LM
KMM	$\xrightarrow{\lambda''_{K\beta}}$	MMM.

Now the rate of decay of single K-shell vacancy (K) states is

$$\frac{-dN_K}{dt} = \lambda_K N_K,$$

so the number of K states remaining at time t is

$$N_K = N_K^0 e^{-\lambda_K t}. \tag{A1}$$

The decay rate of single-K-plus-single-L-shell vacancy (KL) states is

$$\frac{-dN_{KL}}{dt} = (\lambda'_K + \lambda'_L) N_{KL},$$

so the number of KL states remaining at time t is

$$N_{KL} = N_{KL}^0 e^{-(\lambda'_K + \lambda'_L)t}. \tag{A2}$$

The rate of $K\beta$ x-ray emission in the presence of an L-shell vacancy is

$$\frac{dN_{K\beta}^L}{dt} = \lambda'_{K\beta} N_{KL},$$

and hence the total number of $K\beta$ x rays emitted in the presence of an L-shell vacancy is

$$N_{K\beta}^L = \lambda'_{K\beta} N_{KL}^0 \int_0^\infty e^{-(\lambda'_K + \lambda'_L)t}\, dt = \frac{\lambda'_{K\beta}}{\lambda'_K + \lambda'_L} N_{KL}^0. \tag{A3}$$

The total rate of $K\beta$ x-ray emission is

$$\frac{dN_{K\beta}^T}{dt} = \lambda_{K\beta} N_K + \lambda'_{K\beta} N_{KL} + \lambda''_{K\beta} N_{KMM}. \tag{A4}$$

The rate of change of KMM states is given by the differential equation

$$\frac{dN_{KMM}}{dt} = \lambda'_L N_{KL} - \lambda''_K N_{KMM},$$

whose solution gives

$$N_{KMM} = C_1 N_{KL}^0 (e^{-(\lambda'_K + \lambda'_L)t} - e^{-\lambda''_K t}), \tag{A5}$$

where

$$C_1 = \lambda'_L / (\lambda''_K - \lambda'_K - \lambda'_L).$$

Substituting Eqs. (A1), (A2), and (A5) into Eq. (A4) and integrating over all t yields, for the total number of $K\beta$ x rays which are emitted,

$$N_{K\beta}^T = \frac{\lambda_{K\beta}}{\lambda_K} N_K^0 + \left(\frac{\lambda''_K \lambda'_{K\beta} + \lambda'_L \lambda''_{K\beta}}{\lambda''_K (\lambda'_K + \lambda'_L)} \right) N_{KL}^0. \tag{A6}$$

Now let

$$C_2 = (\lambda_K - \lambda'_K)/\lambda_K,$$

$$C_3 = (\lambda_{K\beta} - \lambda''_{K\beta})/\lambda_{K\beta}$$

and assume that the influence of one L-shell vacancy on $\lambda_{K\beta}$, of one K-shell vacancy on λ_L, and of two M-shell vacancies on λ_K are negligible so that

$$\lambda'_{K\beta} = \lambda_{K\beta}, \quad \lambda'_L = \lambda_L, \quad \lambda''_K = \lambda_K.$$

Then Eq. (A6) reduces to

$$N^T_{K\beta} = \frac{\lambda_{K\beta}[\lambda_L + \lambda_K(1-C_2)]N^0_K + \lambda_{K\beta}[\lambda_K + \lambda_L(1-C_3)]N^0_{KL}}{\lambda_K[\lambda_L + \lambda_K(1-C_2)]} \tag{A7}$$

and the fraction of $K\beta$ x rays emitted in the presence of an L-shell vacancy is obtained by dividing Eq. (A7) into Eq. (A3). The final result is

$$\frac{N^L_{K\beta}}{N^T_{K\beta}} = \frac{\lambda_K N^0_{KL}}{[\lambda_L + \lambda_K(1-C_2)]N^0_K + [\lambda_K + \lambda_L(1-C_3)]N^0_{KL}}. \tag{A8}$$

Using the definitions of P_{KL} and g_{KL},

$$g_{KL} \equiv N^L_{K\beta}/N^T_{K\beta},$$

$$P_{KL} \equiv N^0_{KL}/(N^0_K + N^0_{KL}),$$

Eq. (A8), after a little algebraic manipulation, can be rearranged to give

$$P_{KL} = \frac{[(\lambda_K + \lambda_L)/\lambda_K - C_2]g_{KL}}{1 + (C_2 - C_3\lambda_L/\lambda_K)g_{KL}}. \tag{A9}$$

Since the $L_1 \rightarrow L_{2,3}$ Coster–Kronig transition rates are large,[17] we shall assume that the L-shell vacancy always resides in the $L_{2,3}$ subshells. Now the presence of an L-shell vacancy will reduce λ_K *at most* to $\frac{5}{6}$ of its normal value, and so C_2 will be less than about 0.17. The presence of two M-shell vacancies will reduce $\lambda_{K\beta}$ *at most* to $\frac{2}{3}$ of its normal value for Ca and to $\frac{5}{6}$ of its normal value for Fe. Therefore, C_3 should not be more than 0.33 for Ca or more than 0.17 for Fe. As long as g_{KL} is not too large ($\lesssim 0.7$), then the second term in the denominator of Eq. (A9) will be small compared to unity and to a good approximation Eq. (A9) will reduce to

$$P_{KL} = \frac{(\lambda_K + \lambda_L)}{\lambda_K} g_{KL},$$

or

$$P_{KL} = \frac{(\Gamma_K + \Gamma_L)}{\Gamma_K} g_{KL}, \tag{A10}$$

where Γ_K is the total K-shell level width and Γ_L is the level width of the L_3 subshell, since the L_2 subshell width will contain a contribution due to the $L_2 \rightarrow L_3$ Coster–Kronig transitions, where such transitions are energetically possible.

---

*Work supported by the U. S. Atomic Energy Commission and the Robert A. Welch Foundation.

[1]J. D. Garcia, R. J. Fortner, and T. M. Kavanagh, Rev. Mod. Phys. **45**, 111 (1973).
[2]A. R. Knudson, P. G. Burkhalter, and D. J. Nagel, in *Proceedings of the International Conference on Inner-Shell Ionization Phenomena, Atlanta, 1972*, Conf.-720404 (U.S. AEC, Oak Ridge, Tenn., 1973), Vol. 3, p. 1675.
[3]J. S. Hansen, T. K. Li, and R. L. Watson, in Ref. 2, p. 1682.
[4]C. F. Moore, M. Senglaub, B. Johnson, and P. Richard, Phys. Lett. A **40**, 107 (1972).
[5]M. Gryzinski, Phys. Rev. **138**, A336 (1965).
[6]J. M. Hansteen and O. P. Mosebekk, Phys. Rev. Lett. **29**, 1361 (1972).
[7]J. S. Hansen Phys. Rev. A **8**, 822 (1973).
[8]E. Storm and H. I. Israel, Nucl. Data A **7**, 565 (1970).
[9]F. Herman and S. Skillman, *Atomic Structure Calculations* (Prentice-Hall, Englewood Cliffs, N.J., 1963).
[10]C. W. Lewis, R. L. Watson, and J. B. Natowitz, Phys. Rev. A **5**, 1773 (1972).
[11]C. Rugge, R. L. Watson, and J. B. Wilhelmy, Least-Squares Fitting Programs for K X-Ray Pulse-Height Spectra, Lawrence Radiation Laboratory, Berkeley (unpublished).
[12]R. L. Watson, H. R. Bowman, and S. G. Thompson, Phys. Rev. **162**, 1169 (1967).
[13]R. L. Watson and T. K. Li, Nucl. Phys. A. **178**, 201 (1971).
[14]E. J. McGuire, Phys. Rev. A **3**, 587 (1971).
[15]M. H. Chen, B. Crasemann, and V. O. Kostroun, Phys. Rev. A **4**, 1 (1971).
[16]J. H. Scofield, Phys. Rev. **179**, 9 (1969).
[17]W. Bambynek, B. Crasemann, R. W. Fink, H. U. Freund, H. Mark, C. D. Swift, R. E. Price, and P. V. Rao, Rev. Mod. Phys. **44**, 716 (1972).
[18]D. L. Walters and C. P. Bhalla, Phys. Rev. A **4**, 2164 (1971).
[19]M. A. Blokhin, *The Physics of X-Rays*, 2nd ed. (Nauka, Moscow, 1957); Atomic Energy Commission Technical Report. No.–4502. Also see Kenneth D. Sevier, *Low Energy Electron Spectrometry* (Wiley, New York, 1972), pp. 230–233.
[20]L. G. Parratt, Rev. Mod. Phys. **31**, 616 (1959). Also see Kenneth D. Sevier, Ref. 19, pp. 230–233.
[21]J. A. Bearden and A. F. Burr, Rev. Mod. Phys. **39**, 125 (1967).